Environmental Science & Technology

pubs.acs.org/est

Article

Replacement Flame-Retardant 2-Ethylhexyldiphenyl Phosphate (EHDPP) Disrupts Hepatic Lipidome: Evidence from Human 3D Hepatospheroid Cell Culture

Chander K. Negi, Darshak Gadara, Jiri Kohoutek, Lola Bajard, Zdeněk Spáčil, and Ludek Blaha*

Cite This: *Environ. Sci. Technol.* 2023, 57, 2006−2018

Read Online

ACCESS | Metrics & More | Article Recommendations | Supporting Information

ABSTRACT: The present study aims to evaluate the effects of repeated exposure to 2-ethylhexyldiphenyl phosphate (EHDPP) on human liver cells. *In vitro* three-dimensional (3D) hepatospheroid cell culture was utilized to explore the potential mechanisms of EHDPP-mediated metabolic disruption through morphological, transcriptional, and biochemical assays. Lipidomics analysis was performed on the individual hepatospheroids to investigate the effects on intracellular lipid profiles, followed by hepatospheroid morphology, growth, functional parameters, and cytotoxicity evaluation. The possible mechanisms were delineated using the gene-level analysis by assessing the expression of key genes encoding for hepatic lipid metabolism. We revealed that exposure to EHDPP at 1 and 10 μM for 7 days alters the lipid profile of human 3D hepatospheroids. Dysregulation in several lipid classes, including sterol lipids (cholesterol esters), sphingolipids (dihydroceramide, hexosylceramide, ceramide, sphingomyelin), glycerolipids (triglycerides), glycerophospholipids, and fatty acyls, was noted along with alteration in genes including ACAT1, ACAT2, CYP27A1, ABCA1, GPAT2, PNPLA2, PGC1α, and Nrf2. Our study brings a novel insight into the metabolic disrupting effects of EHDPP and demonstrates the utility of hepatospheroids as an *in vitro* cell culture model complemented with omics technology (*e.g.*, lipidomics) for mechanistic toxicity studies.

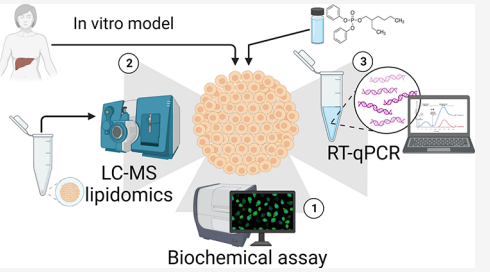

KEYWORDS: *3D spheroids, lipidomics, repeat dose toxicity, metabolic disrupting chemicals, flame retardants*

1. INTRODUCTION

Organophosphate flame retardants (OPFRs) are widely used in several indoor and outdoor products to substitute currently regulated polybrominated diphenyl ethers (PBDEs).[1] OPFR, such as 2-ethylhexyldiphenyl phosphate (EHDPP), is ubiquitously found in various biological samples and environmental matrices, including apartments, houses, primary schools, offices, and cars.[2] Moreover, recent findings from studies in Sweden, Belgian, Norway, and China have found EHDPP in composite food samples at a relatively high level.[3−6] Notably, EHDPP and their metabolites have also been frequently detected in blood and urine samples in the general population.[7,8] It was the second-most detected OPFR with a median concentration of 1.22 ng/mL in human blood in the nonoccupational population in Shenzhen, China.[9] The presence of EHDPP was also detected in deciduae (100% of analyzed samples) with a median concentration of 5.96 ng/g dry weight and a much higher concentration of 13.6 ng/g dry weight in chorionic villi (96%) in pregnant women,[10] suggesting maternal transfer and prenatal exposure to developing embryos. With the ubiquitous presence, it is evident that human exposure to toxicants such as EHDPP is unavoidable and occurs throughout their lifetime. In addition, occupational exposure could be much higher than environmental exposure. Exposure pathways for EHDPP include inhalation, dermal exposure, ingestion of dust, dietary intake, and foodstuff but the dietary intake or ingestion from the food sources seems predominant.[4] The oral intake of EHDPP has been estimated to be higher than 1000 ng/day in the Belgian adult population.[6]

Several health hazards associated with exposure to EHDPP, such as endocrine disruption developmental and neurotoxicity in *in vitro* cell culture and experimental animal models, have already been reported.[11−15] In addition, recent evidence highlights the metabolic disrupting potential of EHDPP in mice, where prenatal exposure affected the metabolic phenotype of male offspring.[16] Comparable effects were also noted in a few other *in vitro* studies, for instance, EHDPP-mediated induction of adipogenesis in mouse 3T3-L1 preadipocytes through the peroxisome proliferator-activated receptor-γ (PPAR-γ) signaling pathway,[17] hepatotoxic effects in human fetal hepatocyte (L02) cells at the level of

Received: June 16, 2022
Revised: December 22, 2022
Accepted: December 22, 2022
Published: January 24, 2023

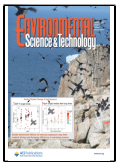

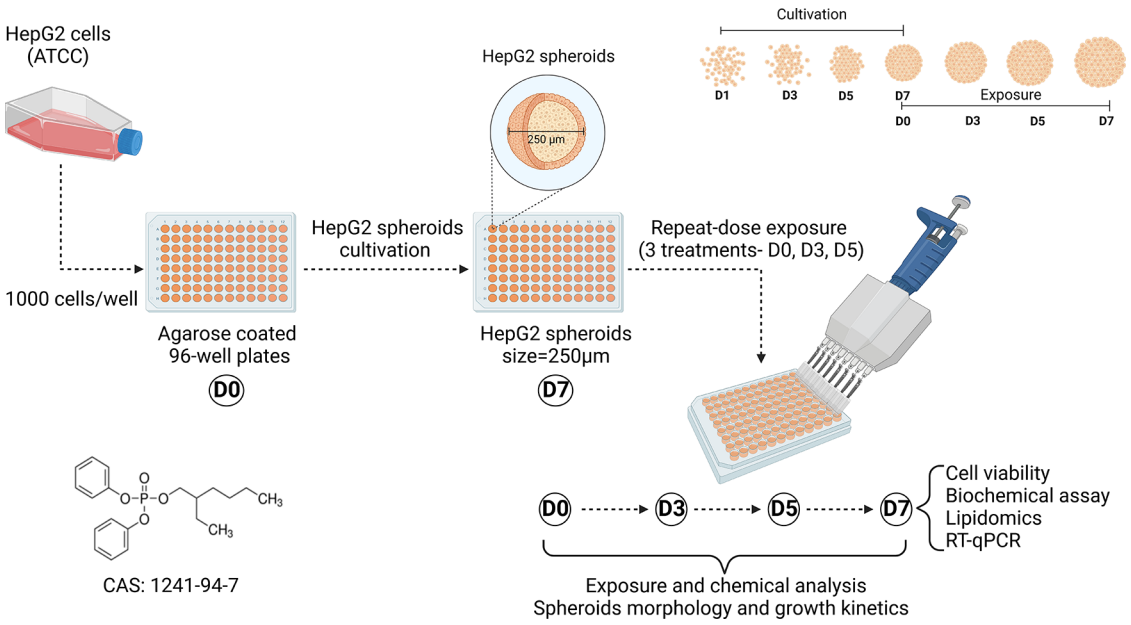

Figure 1. HepG2 spheroid culture and exposure scheme. One thousand viable cells were seeded into 1.5% agarose-coated 96-flat-bottom well plates and were cultivated at a 37 °C humidified incubator with 5% CO_2 and maintained for 14 days. The culture medium was refreshed every 3−4 days. Treatments started on D7 (mean diameter of spheroids: 250−300 μm). Treatment was performed every second to third day, and the hepatospheroids were repeatedly exposed for 7 days (three exposures). The concentration of DMSO was maintained at 0.01% at all experimental conditions. Spheroid growth was monitored using a phase-contrast microscope (BioTek) during every treatment duration.

transcriptome,[18] *etc.* Moreover, the urinary concentrations of EHDPP and its metabolites were found to be associated with increased plasma total cholesterol (TC) and triglyceride (TG) levels in humans.[19] These studies point toward the metabolic disrupting effects of EHDPP, which needs further research attention. However, at the same time, research on potential toxic effects and associated mechanisms in human-based models is scarce.

Occupational and environmental exposures to chemicals are well known to cause hepatotoxicity and liver injury. Environmental contaminants may contribute to the development and progression of various metabolic disease pathologies, such as nonalcoholic fatty liver disease (NAFLD) characterized by increased TG accumulation, and more severe phenotypes such as nonalcoholic steatohepatitis (NASH).[20] However, the underlying mechanisms linking chemical exposure with metabolic pathologies remain poorly understood. Identification of liver lipid biomarkers may serve as an efficient strategy to characterize biological responses and early identification of potential targets of these emerging compounds leading to the identification of possible hazards and a better understanding of the toxicological mechanisms. With the emergence of omics technologies such as lipidomics in toxicology, potential effects on phenotypes can be established by liking molecular descriptors such as gene−protein−lipid/metabolite, *etc.*, using the *in vitro* settings. In our previous study, we utilized an adverse outcome pathway (AOP)-based screening approach to identify and characterize the steatogenic potential of nine OPFR, including EHDPP. We found increased lipid accumulation and expression of lipid metabolism-related genes in human HepG2 monolayer cell culture at low micromolar concentrations,[21] and our in silico analysis identified pregnane X receptor (PXR) and/or PPAR-γ as the potential molecular initiating events (MIEs). However, modulations of specific lipid classes or the long-term repeated low-dose exposure effects of EHDPP remain elusive. In general, it remains unknown which lipid classes could potentially be altered by long-term repeated exposure, which is important and relevant to human populations. Moreover, the repeated exposure effects of low doses are particularly of great interest also for the safety assessment of chemicals. As *in vitro* long term, repeated exposure studies are difficult to conduct using conventional human hepatocyte monolayer cultures due to rapid dedifferentiation and subsequent loss of hepatocyte function.[22] Therefore, in the present study, we utilized the *in vitro* three-dimensional (3D) hepatospheroid cell culture for repeated dose exposure. The HepG2 3D hepatospheroid models are well characterized, metabolically competent, and demonstrated to have improved liver-like properties, including the increased expression of albumin, urea, xenobiotic transcription factors, phase I and II metabolism enzymes, and transporters.[23] In addition, higher cytochrome P450-mediated metabolism in comparison to monolayer cultures has also been noted.[23]

The present study investigates the detailed mechanisms of EHDPP-mediated adverse metabolic effects by characterizing the hepatic lipid profiles in a human liver 3D spheroid cell culture. We measured hepatospheroid cytotoxicity, morphological and growth kinetics, hepatocyte functional parameters like albumin and urea release, and reactive oxygen species (ROS) production after EHDPP exposure. We quantified 216 different lipid species, including fatty acyls, sterols, glycerolipids, glycerophospholipids, and sphingolipids, using liquid chromatography with tandem mass spectrometry (LC-MS/MS) lipidomics platform. In addition, we delineate the molecular mechanisms for EHDPP-mediated alteration in lipid metabolism using gene-level transcriptional analysis.

2. MATERIALS AND METHODS

2.1. Cell Culture and Hepatospheroid Generation. Human hepatoma cells (HepG2) purchased from American Type Culture Collection (ATCC, Manassas, VA) were grown

https://doi.org/10.1021/acs.est.2c03998
Environ. Sci. Technol. 2023, 57, 2006−2018

in minimum essential media (MEM) (Gibco, NY) supplemented with 0.11 g/L of sodium pyruvate (Sigma-Aldrich), 1.50 g/L of $NaHCO_3$ (Sigma-Aldrich), 1% of nonessential amino acids (Gibco), and 10% of fetal bovine serum (Biosera) at 37 °C in a humidified atmosphere of 95% air and 5% CO_2 (v/v). Cells were subcultured at an 80−90% confluency. Confluent cells were trypsinized (0.05% trypsin/0.53 mM ethylenediaminetetraacetic acid (EDTA)) and passaged every 6−7 days. For the generation of hepatospheroids, 1000 viable cells were seeded into 1.5% of agarose (Sigma-Aldrich)-coated 96-flat-bottom well plates (TPP) and grown in a 37 °C humidified incubator with 5% CO_2 till 14 days (7 days of cultivation and 7 days of exposure). The culture medium was refreshed every 3−4 days. Agarose is biocompatible and strongly resists cell adhesion. Therefore, suspension cells settle into discrete populations of equivalent numbers for cells of uniform-sized spheroids.[24] All experiments were performed using the standard aseptic techniques in a biosafety cabinet and were repeated at least three times unless otherwise specified.

2.2. Chemical Exposure and Quantification. 2-Ethylhexyldiphenyl phosphate (purity, >90.0%) chemical abstract service (CAS) number 1241-94-7 was purchased from the Tokyo Chemical Industry (TCI, Europe), and the chemical stock was prepared by dissolving in dimethyl sulfoxide (DMSO) (Sigma-Aldrich) and stored at −20 °C. On day 7 of incubation, hepatospheroids of a regular size (≈250−300 μm) were repeatedly exposed to nominal concentrations, *i.e.*, 1, 10, or 50 μM of freshly prepared EHDPP for 7 days, and 0.01% v/v of DMSO was tested as the solvent control (SC). Treatment was performed every second to third day (three exposures during 7 days of experiments), as depicted in the experimental design (Figure 1). The spheroid cell culture supernatants from each treatment group were collected and stored at −80 °C until further analysis. The samples for chemical analysis of EHDPP were collected on every exposure day and analyzed using an Agilent 1290 Infinity liquid chromatography (LC) system, as described previously[21] and also in Section S1.1, Supporting Information.

2.3. Hepatospheroid Morphology and Growth Kinetics. The hepatospheroid morphology, integrity, diameter, area, circularity, and translucency were measured before exposure on day 7 (D0) and then on days D3, D5, and D7 using brightfield microscopy (BioTek). Image analysis was done using the BioTek inbuilt image analysis tool.

2.4. Cell Viability Analysis. Cell viability was determined by the CellTiter-Glo 3D Cell Viability Assay as per the manufacturer's protocol and qualitatively assessed through fluorescent staining using a mixture of dyes: calcein acetoxymethyl ester (calcein-AM) and propidium iodide. For staining, the exposure media was removed, and spheroids were incubated at 37 °C and 5% CO_2 for 30 min with a mixture of 2 μM solution of calcein-AM and 4 μM propidium iodide prepared in sterile phosphate-buffered saline (PBS). Images were then taken with Cytation 5 (BioTek instruments). Lactate dehydrogenase (LDH) assay was also performed using Cytotoxicity Detection Kit (Roche, U.K.) following the manufacturer's protocol, and absorbance at 490 nm was measured using a Synergy2 microplate reader (BioTek, VT).

2.5. Albumin and Urea Production. Albumin production was assessed using enzyme-linked immunosorbent assay (ELISA) using the Human Albumin DuoSet ELISA kit (R&D systems). Urea production was quantified by QuantiChrom Urea Assay Kit (BioAssay Systems Hayward, CA). The absorbance values at 405 nm were measured with a Synergy2 microplate reader (BioTek, VT).

2.6. Lipidomics Analysis. Each spheroid was collected and washed three times with ice-cold PBS. After a brief vortex, the remaining PBS was aspirated. Lipids were extracted by adding 60 μL of isopropanol (Biosolve) with a mixture of 16 lipid internal standards (SPLASH Lipidomics; cat. #330707) and sphingolipid internal standards (Cer/Sph Mixture I, Avanti Polar Lipids, Alabaster, cat. #LM6002) (Table S1, Supporting Information). Samples were sonicated (10 min), vortexed (10 min), and centrifuged (5 min). The supernatant (45 μL) was transferred into a vial with glass inserts for the LC-MS analysis using a 1290 Infinity II UHPLC (Agilent) system coupled to a 6495 Triple Quadrupole mass spectrometer (Agilent). The protein pellet was dried in a SpeedVac vacuum concentrator (Savant SDP121 P, Thermo Fisher Scientific). The dried pellet was reconstituted in the buffer (1% sodium dodecyl sulfate (SDS), 150 mM NaCl, 50 mM tris, pH 7.8), and the protein concentration was quantified using bicinchoninic acid (BCA) assay (Thermo Fisher Scientific) as per the manufacturer's protocol (see Section S1.2, Supporting Information, for detailed methods for lipidomics analysis).

2.7. ROS Detection by H_2O_2 Assay. The ROS-Glo H_2O_2 Assay (Promega Inc., Madison, WI) was used to measure the hydrogen peroxide (H_2O_2) level. The spheroids were incubated with 25 μM of H_2O_2 substrate solution for 6 h (last 6 h exposure) at 37 °C and 5% CO_2. After the incubation period, 50 μL of media was transferred to another plate, and an equal volume of ROS-Glo detection solution was added. The plate was incubated for 20 min at room temperature, and relative luminescence was recorded using a BioTek microplate reader.

2.8. RNA Extraction and Real-Time Quantitative Polymerase Chain Reaction (RT-qPCR). Spheroids were pooled before RNA extraction to generate sufficient input material for complementary DNA (cDNA) synthesis. Total RNA was extracted using RNeasy Mini Kit (Qiagen Inc., Mississauga, ON), and the quality/purity was ensured by observing the UV absorbance 260/280 nm ratio using a nanodrop spectrophotometer (Thermo Scientific). Total RNA was then reverse-transcribed using SensiFAST cDNA Synthesis kit (Bioline, London, U.K.). The resulting cDNA was amplified by RT-qPCR using SYBR Green PCR Master Mix in a 10 μL reaction (5 μL SensiFAST SYBR No-ROX Kit (Bioline, London, U.K.), 0.4 μL qPCR primers (forward and reverse 4 μM), 1 μL cDNA, 3.2 μL nuclease-free water) using Roche 480 LightCycler (Roche, Basel, Switzerland). Expression of the following genes encoding for lipid metabolism was analyzed: glycerol-3-phosphate acyltransferase 2 (GPAT2), lipin 1 (LPIN), patatin-like phospholipase domain containing 2 (PNPLA2), diacylglycerol *O*-acyltransferase 2 (DGAT2), carbohydrate-responsive element-binding protein (ChREBP), mitochondrial β-oxidation, *i.e.*, acylcarnitines palmitoyl-transferase 1α (CPT1α), peroxisome proliferator-activated receptor (PPAR-γ), acetyl-coenzyme A acetyltransferase (ACAT1 and ACAT2), 3-hydroxy-3-methylglutaryl-CoA reductase (HMGCR), 3-hydroxy-3-methylglutaryl-CoA synthase 1 (HMGCS1), bile acid biosynthesis (CYP27A1 and CYP7A1), oxidative stress or antioxidant status, nuclear factor erythroid 2-related factor 2 (Nrf2), peroxisome proliferator-activated receptor γ coactivator 1-α (PGC1α), and ATP binding cassette subfamily A member 1 (ABCA1). Validated

https://doi.org/10.1021/acs.est.2c03998
Environ. Sci. Technol. 2023, 57, 2006−2018

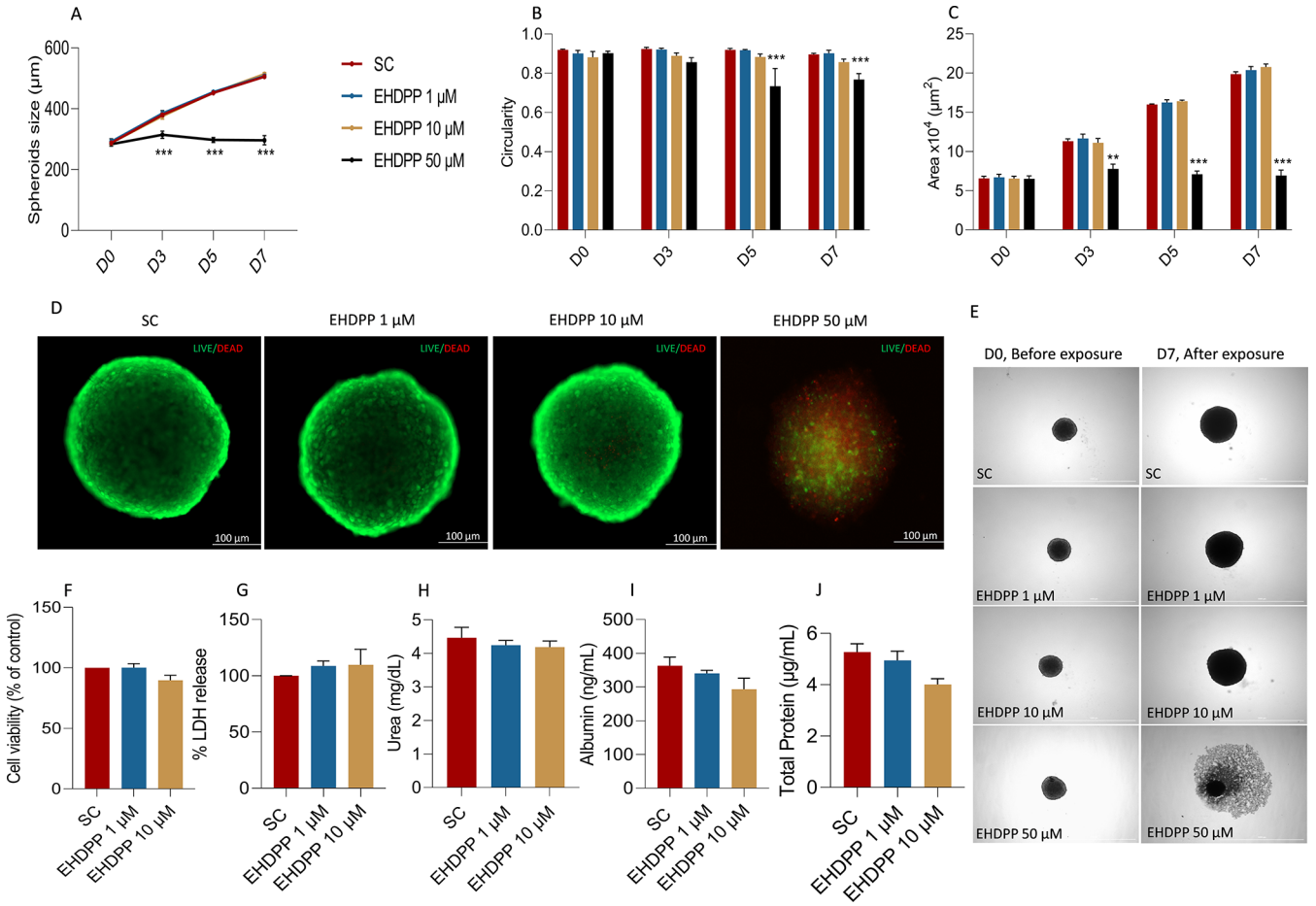

Figure 2. Morphological assessment and growth kinetics of hepatospheroids. Quantitative evaluation of hepatospheroid morphology: (A) spheroid size (diameter), (B) spheroid area, and (C) circularity. (D) Representative photomicrograph showing cell viability of hepatospheroids using live/dead staining with calcein-AM (live cell indicator) and propidium iodide (dead cell indicator). Images were taken in BioTek Cytation 5 with fluorescence microscopy mode, using green fluorescence protein (GFP) and Texas red (TR) filter. Scale bar, 100 μm. (E) Representative photomicrographs (brightfield) showing morphological differences between hepatospheroids exposed repeatedly to EHDPP (1, 10, 50 μM) and SC on D0 before exposure and D7 after exposure. (F) Endpoint cell viability was determined by CellTiter-Glo luminescent and (G) LDH release assay after 7 days of exposure with EHDPP (1 and 10 μM). (H) Urea, (I) albumin, and (J) total protein (n = 10 spheroids) as hepatic function parameters after 7 days of exposure to EHDPP 1 and 10 μM or SC. Data presented as mean ± SEM of three to four independent experiments. Significance was determined by one-way ANOVA, $^{**}p < 0.01$; $^{***}p < 0.001$.

primers were used for the reaction, and sequences are presented in Table S2, Supporting Information. The RT-qPCR conditions were set at 95 °C for 2 min, and 40 cycles of 5 s at 95 °C, 10 s at 60 °C, and 20 s at 72 °C, melt curve: 5 s at 95 °C, 1 min at 55 °C. Melting curve analysis was carried out to confirm the specificity of RT-qPCR products. The expression levels of target genes were normalized to two endogenous controls: eukaryotic translation elongation factor 2 (EEF2) and malate dehydrogenase 1 (MDH1) mRNA levels by the geometric mean of the Cq values of both genes. The relative mRNA levels of genes were quantified according to Livak and Schmittgen's method.[25]

2.9. Data Analysis and Statistics. All data are expressed as the mean ± standard error of the mean (SEM) (n = 3−4 independent experiments). All statistical analysis was performed using GraphPad Prism version 9 for Windows (GraphPad Software, La Jolla, California, www.graphpad.com). Analysis of variance (ANOVA) followed by Dunnett's multiple comparison test was performed for statistical differences between two or more groups of the data. p-Values are indicated by asterisks: $^{*}p < 0.05$, $^{**}p < 0.01$, and $^{***}p < 0.001$.

3. RESULTS

3.1. Concentrations and Stability of EHDPP in Exposure Media. The stability of EHDPP and nominal tested concentrations were verified in the exposure media using the LC-MS/MS method. Since the media was refreshed on the third and fifth days, the concentration was measured after 72 and 48 h of exposure. Measured concentrations of EHDPP at nominal 1 μM (359.67 ng/mL) and 10 μM (3596.65 ng/mL) were 180.37 ± 2.9 and 1717.92 ± 21.25 after 72 h (D3) and 330.42 ± 2.79 and 3054.83 ± 36.11 ng/mL after 48 h (D5) in culture media. This represents approximately 50 and 80% of the nominal concentration after 72 and 48 h of exposure, respectively. The concentration of EHDPP thus remained within 50−80% of the nominal concentration throughout the exposure duration. For simplicity, all results are expressed as nominal concentrations.

3.2. Effects on Morphology and Growth Kinetics. Initially, we evaluated the effects of repeated exposure to three

https://doi.org/10.1021/acs.est.2c03998
Environ. Sci. Technol. 2023, 57, 2006−2018

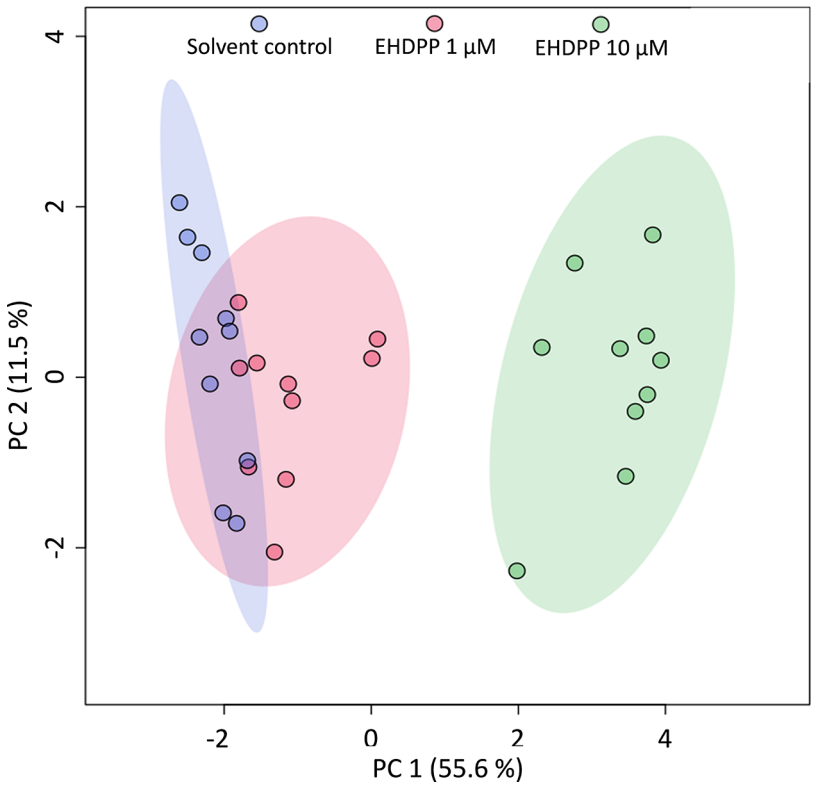

Figure 3. PCA score plot of the lipid profile of 3D hepatospheroids treated with EHDPP 1 and 10 μM or SC for 7 days.

concentrations of EHDPP, *i.e.*, 1, 10, and 50 μM or SC, on the morphology and growth kinetics of hepatospheroids. EHDPP 50 μM arrested the growth of the spheroids (diameter and area of spheroids reduced), affected circularity, reduced translucency, disintegrated spheroids, and increased the necrotic area over time (Figure 2E). This observation indicates that EHDPP at higher concentrations is toxic and affects the morphology and growth kinetics of spheroids. At the same time, no significant changes in the spheroid growth pattern and morphology at 1 and 10 μM groups were observed (Figure 2). This observation indicates that these concentrations might not be cytotoxic to the hepatospheroids.

3.3. Effects on Cell Viability and Hepatocyte Function. Cell viability was further evaluated using calcein-AM and propidium iodide staining. Propidium iodide staining was used for the identification of apoptotic/necrotic cells in the spheroids, while calcein-AM indicates the live cells. Treatment with EHDPP 50 μM induced cytotoxicity, as visualized by the increased propidium iodide staining, while 1 and 10 μM did not (Figure 2). We also evaluated the cytotoxicity by the LDH release method and CellTiter-Glo luminescent assay, and no significant changes were observed at 1 and 10 μM in both assays (Figure 2F,G). No significant change in the level of albumin and urea was observed, indicating normal and stable hepatocyte function. The spheroids continued to secrete albumin and urea throughout the exposure duration, and no significant difference (mean ± SEM) in secreted albumin and urea was observed between EHDPP 1, 10 μM, and SC (Figure 2H,I).

3.4. Effects on Hepatic Lipidome and Metabolic Pathways. Lipidomics analysis was performed to investigate the effects of EHDPP on hepatospheroid lipid profile. In total, 216 individual lipid species were relatively quantified based on their MS/MS spectra. The identified lipid species (major lipid categories) were further sorted into five lipid classes according to the lipid metabolites and pathways strategy (LIPID MAPS) consortium[26] (Table S3, Supporting Information). The principal component analysis (PCA) score plot separates three treatment groups—EHDPP 1, 10 μM, or SC (Figure 3). As depicted in Figure 4 the levels of several lipid subclasses were significantly altered in the EHDPP treatment group. A significant decrease in acylcarnitine (CAR) was observed (Figure 4A) within the fatty acyl category. In total, 52 lipids from the glycerolipid category were quantified, 12 diacylglycerols (DG) and 40 triacylglycerols (TG). Total TG was significantly upregulated in the EHDPP treatment group, while no significant change in the total DG was observed. Moreover, the ratios of concentrations of TG/DG were significantly increased in the EHDPP 10 μM treatment group (Figure 4C). Trends among the glycerophospholipid subclasses varied. Phosphatidylethanolamines (PEs), alkylphosphatidylcholine (PC-O), lysophosphatidylcholine (LPC), lysophosphatidylethanolamines (LPEs), and phosphatidylinositol (PI) were significantly increased, while no significant changes in phosphatidylcholine (PC), alkenylphosphatidylcholine (PC-P), phosphatidylglycerol (PG), and phosphatidylserine (PS) species were observed. In addition, the EHDPP treatment significantly decreased the ratios of concentrations of PC/PE (Figure 4G). Since these are the most abundant phospholipids in all mammalian cell membranes, this might indicate altered cell membrane homeostasis after EHDPP exposure. Among all PS species, (PS 34:2, 36:2, 38:3, 38:4, and 40:7) showed a decreasing trend; however, PS 40:6 was significantly induced upon the EHDPP treatment (Figure S1, Supporting Information). All phosphatidylinositol (PI) species were upregulated in the EHDPP treatment group. Among 14 PIs, PI 38:3 was significantly downregulated upon the EHDPP treatment (Figure S2, Supporting Information). Sphingolipid

https://doi.org/10.1021/acs.est.2c03998
Environ. Sci. Technol. 2023, 57, 2006−2018

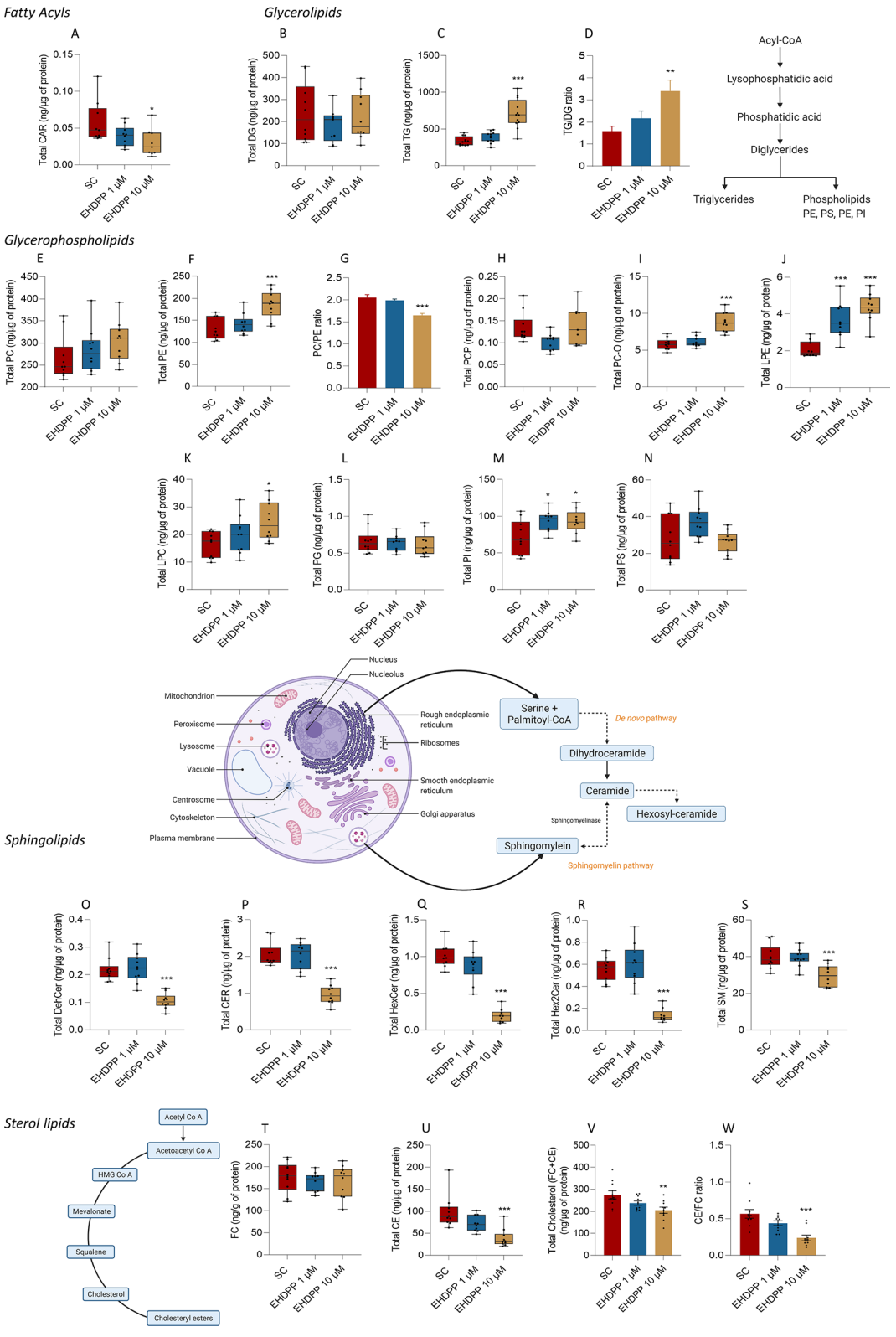

Figure 4. Targeted lipidomic analysis of hepatospheroids exposed to EHDPP (1 and 10 μM) or SC for 7 days. (A) Acylcarnitines (CAR), (B) diglyceride (DG), (C) triglyceride (TG), (D) TG:DG ratio, (E) phosphatidylcholine (PC), (F) phosphatidylethanolamines (PEs), (G) PC/PE ratio, (H) alkenylphosphatidylcholine (PC-P), (I) alkylphosphatidylcholine (PC-O), (J) lysophosphatidylethanolamines (LPEs), (K) lysophosphatidylcholine (LPC), (L) phosphatidylglycerol (PG), (M) phosphatidylinositol (PI), (N) phosphatidylserine (PS), (N) phosphatidylethanolamines (PEs), (O) dihydroceramides (dhCer), (P) ceramide (CER), (Q) hexosylceramide (HexCer), (R) hexosylceramide (Hex2Cer), (S) sphingomyelin (SM), (T) free cholesterol (FC), (U) cholesterol esters, (V) total cholesterol, and (W) CE/FC ratio. Statistical significance was evaluated by one-way ANOVA post-Dunnett's multiple comparison test. *$p < 0.05$; **$p < 0.01$; ***$p < 0.001$ ($n = 10$ spheroids/group).

https://doi.org/10.1021/acs.est.2c03998
Environ. Sci. Technol. 2023, 57, 2006−2018

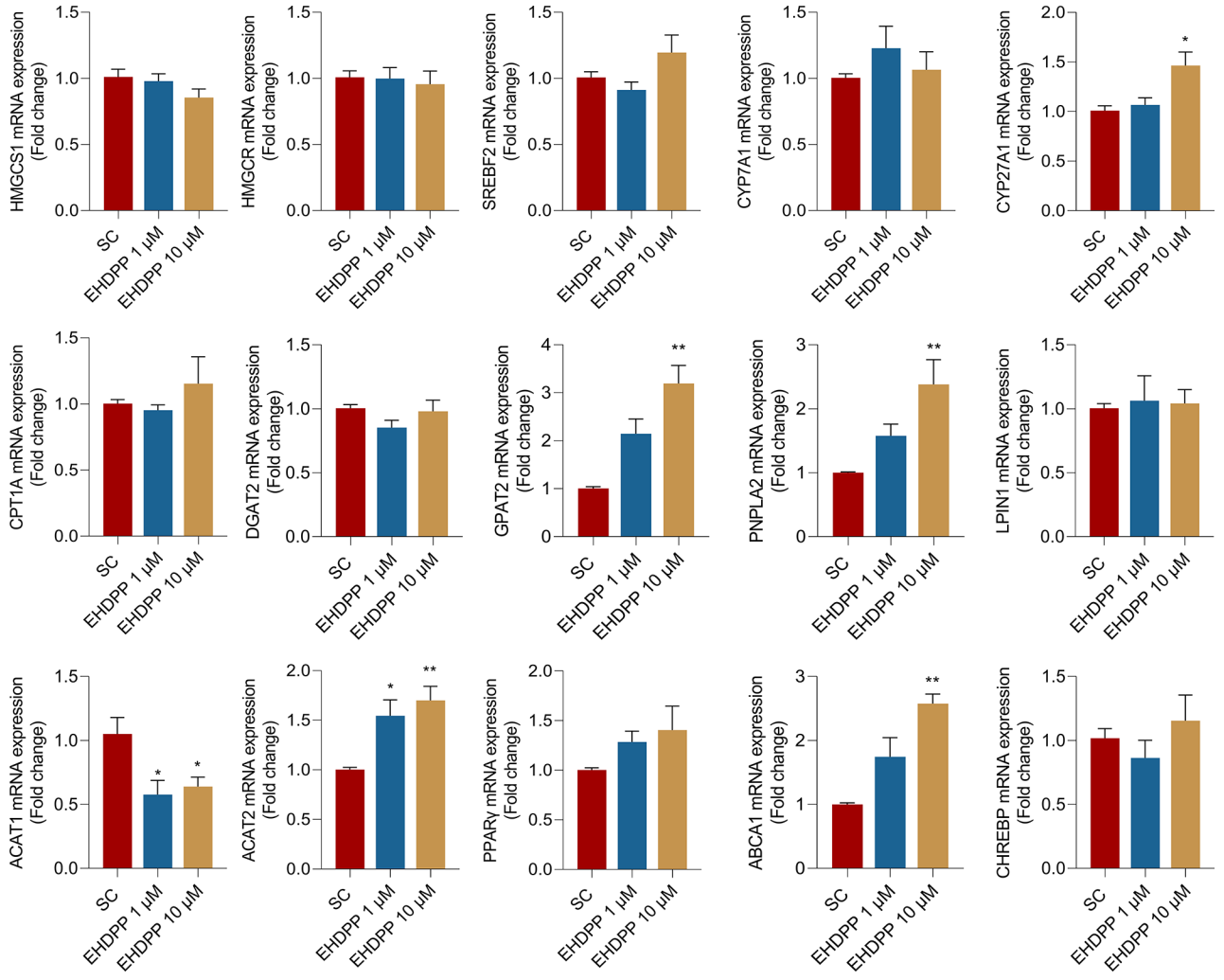

Figure 5. mRNA expression of key genes associated with hepatic lipid metabolism. For all statistical plots, the data are presented as mean ± SEM of three to four independent experiments. Statistical significance was evaluated by ANOVA followed by Dunnett's multiple comparison test. *p < 0.05; **p < 0.01.

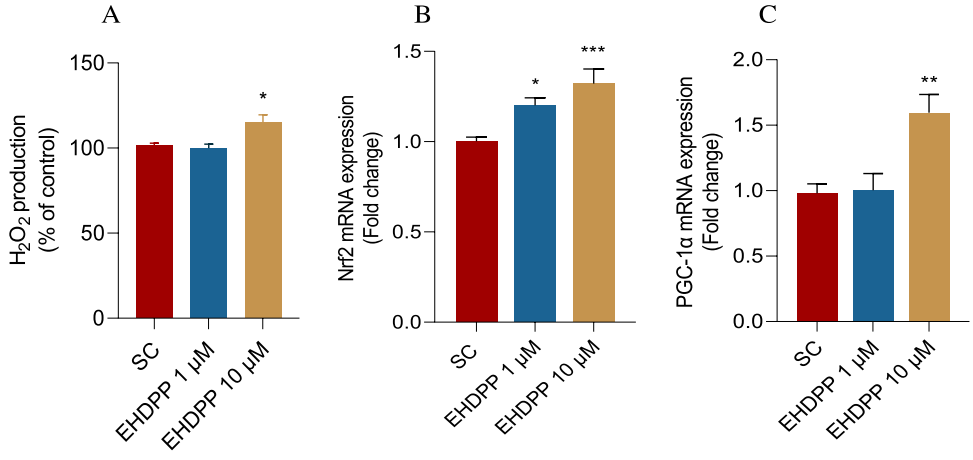

Figure 6. Cellular ROS production and mRNA expression of Nrf2 transcription factor. (A) Elevated ROS production in hepatospheroids treated with EHDPP (1 and 10 μM) or SC for 7 days; mean ± SEM of three independent experiments (n = 3). (B) mRNA expression of Nrf2 and (C) PGC1α; mean ± SEM of four independent experiments. *p < 0.05; **p < 0.01; and ***p < 0.001.

such as ceramide (CER) was significantly decreased; moreover, the precursor in the *de novo* synthesis pathway, *i.e.*, dhCer, also showed a decreasing trend (Figure 4). It was also accompanied by a significant decrease in HexCer, Hex2Cer, and sphingomyelin (SM). However, the analysis of all SM revealed a significant increase of SM 40:3 lipid in the EHDPP treatment group (Figure S3, Supporting Information). The sterol ester cholesteryl ester (CE) was also downregulated significantly.

https://doi.org/10.1021/acs.est.2c03998
Environ. Sci. Technol. 2023, 57, 2006−2018

Although a decreasing trend in free cholesterol (FC) was observed, which was not statistically significant, total cholesterol (FC + CE) was significantly decreased (Figure 4V). Moreover, the CE-to-FC concentration ratio showed a significant decrease from the control, indicating the deficient conversion of FC to CE (Figure 4W).

3.5. Effects on Transcriptional Regulation of Lipid Metabolism. To understand the molecular mechanism underlying EHDPP-induced lipid dysregulation, we measured the expression of key genes encoding for hepatic lipid metabolism, including glycerophospholipids, TG metabolism, cholesterol biosynthesis, uptake, and utilization (oxysterol or bile acid synthesis, *etc.*). EHDPP treatment significantly increased the genes responsible for glycerolipid and glycerophospholipid metabolism, such as GPAT2 and PNPLA2, indicating increased glycerolipid and glycerophospholipid levels, while no significant change in the DGAT2 mRNA levels was observed. No significant change in the expression of genes encoding for *de novo* cholesterol biosynthesis, such as HMGCS1, HMGCR, and SREBF2, was observed (Figure 5). However, the genes responsible for oxysterols or bile acid metabolism (CYP27A1 and ACAT2) were significantly upregulated, while ACAT1 was significantly downregulated. These data suggest that EHDPP might affect the sterol utilization or bile acid metabolism pathway rather than sterol biosynthesis. The mRNA levels of PPAR-γ activated genes such as PGC1α and ABCA1 showed a significantly increasing trend, while no significant change in the CPT1α, CYP7A1, LPIN1, ChREBP, and PPAR-γ was observed (Figure 5).

3.6. Effects on Oxidative Homeostasis. Treatment with EHDPP significantly increased the production of H_2O_2, indicating possible oxidative disbalance, with the effect more pronounced and statistically significant at 10 μM (Figure 6A). Moreover, a significantly increased mRNA expression of transcription factor Nrf2 and coactivator PGC1α was observed, which indicates a possible disturbance in oxidative homeostasis and mitochondrial activity and/or function (Figure 6).

4. DISCUSSION

Exposure to environmental chemicals is an established risk factor for the development and progression of several metabolic diseases, including NAFLD, and lipids play an essential role in the etiology.[27] We previously demonstrated that OPFRs, including EHDPP, could induce lipid accumulation *in vitro* in human liver (HepG2) cell culture, potentially through the nuclear receptor PXR and/or PPAR-γ.[21] These nuclear receptors have been described as potential molecular initiating events (MIEs) leading to the activation of subsequent key events in the AOP for liver injury.[28] The PPAR-γ agonistic activity of EHDPP has also been shown in several other studies.[17,29] The main objective of the present study was to investigate the effects of repeated exposure to EHDPP on human liver 3D cell culture and to characterize the alteration in hepatic lipid profile. The *in vitro* models, such as 3D hepatospheroid cultures, express several physiological characteristics and resemble more to the liver.[30] They sufficiently mimic the *in vivo* conditions and are predictive for toxicants or chemical-induced hepatic toxicities.[30,31]

Initially, we evaluated the hepatospheroid morphology and growth kinetics after EHDPP exposure. EHDPP 1 and 10 μM neither caused any significant morphological dysfunction nor affected the hepatocyte function parameters, whereas 50 μM arrested the growth and affected the morphological parameters of the spheroids. Cell viability assessment, morphological parameters, as well as functional assays for albumin and urea secretion demonstrated 1 and 10 μM of EHDPP to be subcytotoxic. The investigated concentrations 1 and 10 μM (359 and 3596 ng/mL), measured in the culture media after 72 and 48 h, remained within 50 and 80% ranges, respectively. This indicates partial degradation of EHDPP in culture media, but the lower actual exposures remained biologically effective and caused changes in lipid profiles. A similar pattern of EHDPP metabolization has been reported in other cell culture studies, such as chicken embryonic hepatocyte and growth media.[32] Possible metabolites formed from EHDPP have been previously characterized in human liver microsomes,[33] and these could eventually contribute to the observed effects. We quantified 216 different lipid species and demonstrated that subcytotoxic concentrations of EHDPP disrupt the lipid profile of 3D hepatospheroids. The dysregulated lipids are from the class of fatty acyls, sterol lipids, glycerolipids, glycerophospholipids, and sphingolipids. A significant decrease in CAR was observed, which influences metabolic processes through mitochondrial free fatty acid transport and oxidation.[34,35] A decrease in CAR suggests disturbed fatty acid transport and subsequent oxidation in hepatospheroids in response to EHDPP exposure. Several studies have also demonstrated the antioxidant properties of CAR in hepatocytes.[36,37] Therefore, a decrease in CAR also emphasizes the possible oxidative disbalance after EHDPP exposure, which was also previously noted at the transcription level in chicken embryonic hepatocytes.[32]

Glycerolipids such as TG were significantly increased, while no significant difference was noted in DG species. Moreover, the mean TG/DG (product/precursor) ratio was significantly increased, indicating enhanced TG accumulation or defective disposal or redistribution. Interestingly, lipidome analysis of human NAFLD and NASH also exhibited a significantly increased ratio of concentrations of TG/DG.[38] Our gene expression analyses also indicated the increased expression of glycerophospholipids and TG genes such as GPAT2 and PNPLA2. In agreement with our gene expression analysis, a significant increase in the glycerophospholipid species was also observed. These include PC-O, LPC, PE, LPE, and PI, while no significant change in PC, PC-P, and PG species was observed. While most PS species (PS 34:2, 36:2, 38:3, 38:4, 40:7) were suppressed, PS 40:6 was significantly induced upon EHDPP treatment. A similar observation was noted in a recent study where lower-chain PS species (*e.g.*, PS 36:4, 38:5, 38:4, 38:3) were declined, while PS 40:6 was induced in C57BL/6 J mice NASH liver.[39] PS plays a vital role in several intracellular signaling pathways and is also a precursor for other phospholipids.

PC and PE are the major phospholipids in mammalian membranes and are predominantly present on the outer and inner membranes of the plasma bilayer, respectively.[40] The hepatic PC/PE ratio is a key regulator of cell membrane integrity; abnormally high or abnormally low cellular PC/PE ratios can influence energy metabolism in various organelles and have been linked to disease progression in numerous tissues.[41] The decreased ratios of concentrations of PC/PE have been shown to affect membrane integrity leading to the progression from steatosis to NASH in mice and clinically in human NASH.[42] In the present study, a significant decrease in the PC/PE ratio compared to that of the controls was observed, which may indicate the disruption of cell membrane

https://doi.org/10.1021/acs.est.2c03998
Environ. Sci. Technol. 2023, 57, 2006−2018

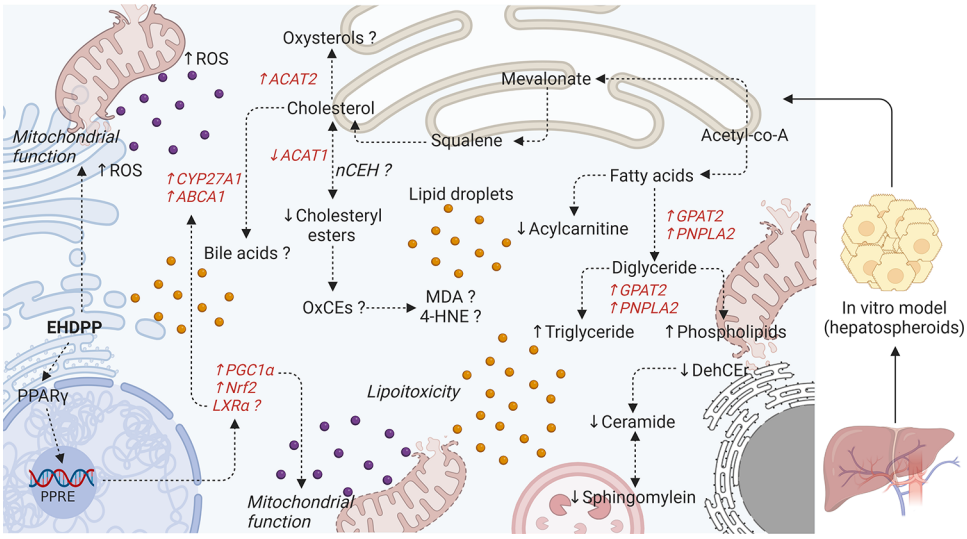

Figure 7. Summary of proposed mechanisms for EHDPP-induced hepatic lipid metabolism dysregulation.

integrity and process related to the progression from steatosis into NASH.

LPC is an essential mediator of hepatic lipotoxicity; it is generated from PC by lipoprotein-bound phospholipase A2 (PLA2).[43] LPC has been demonstrated to induce lipotoxicity, hepatocyte apoptosis, and ER stress *in vitro* in human Huh-7 cells.[44] LPC in the micromolar range has been shown to modulate the mitochondrial microenvironment, including decreased hepatic fatty acid oxidation rate and disruption of mitochondrial integrity and function in mice primary hepatocytes.[45] LPE is the partial hydrolysis product of PE and is also synthesized by PLA2; their precise role in liver disorders is not well studied and is still emerging. A recent study reported that LPE supplementation induces enhanced cellular lipid droplet formation and increased lipid profiles, including TG-, CE-, PE-, LPE-, and PC-containing linoleic acyl triacylglycerol in human liver-derived cell line C3A.[46] The increased LPC and LPE contents observed in the present study could be potentially attributable to increased biosynthesis or increased PLA2 activity, which needs further studies.

PI is the precursor of phosphoinositide, which play a central role in cellular signaling and is responsible for cell proliferation, survival, and metabolism. Besides, it mediates many cellular activities like cell migration, endocytosis, membrane dynamics, *etc.*[47] All PI species were upregulated in the EHDPP treatment group. However, PI 38:3 was significantly downregulated. PI alters cholesterol homeostasis, inhibits CE production, and stimulates reverse cholesterol transport, resulting in the excretion of cholesterol.[48]

Sphingolipids represent one of the major classes of essential cellular lipids that function as structural membrane components and signaling molecules.[49] EHDPP treatment drastically affected sphingolipid metabolism. Total CER was significantly decreased; moreover, in the *de novo* synthesis pathway (Figure 4), *i.e.*, dhCer also showed a decreasing trend. It was also accompanied by a significant decrease in the further metabolites of CER, such as HexCer, Hex2Cer, and SM. CER regulates cellular processes, including cell survival, proliferation, apoptosis, protein synthesis, and autophagy.[50] It has been reported that CER and polyunsaturated phospholipids are strongly reduced in human hepatocellular carcinoma.[51] Alteration in the EHDPP-mediated CER profile might indicate dysfunction/alteration of autophagy and/or apoptosis pathways. Autophagy is the main lysosomal catabolism process, and the mammalian/mechanistic target of rapamycin complex 1 (mTORC1), a serine/threonine kinase, is a well-conserved negative regulator of autophagy.[52] Therefore, the decrease in the lysosomal sphingolipids such as CER upon EHDPP treatment could potentially be mediated by the mTORC1 activity. Moreover, diminished sphingolipid metabolism has been linked with type 2 diabetes pathogenesis in humans, insulin resistance, and impaired pancreatic β cell function in mouse models.[53] EHDPP-mediated defects in the sphingolipid metabolism pathway might indicate a risk of the possible development of diabetes and related secondary complications.

EHDPP treatment significantly reduced the esterified cholesterol (CE) pool, whereas FC levels did not change. However, the total cholesterol (estimated as the sum of FC and CE) also showed significant downregulation. In addition, mRNA levels of PPAR-γ-activated genes such as ABCA1 and PGC1α also increased, indicating PPAR-γ agonistic activity of EHDPP treatment, which was also demonstrated in other studies.[17,29] Moreover, CEs are also being oxidized under certain circumstances leading to a substantial loss of free and esterified cholesterol, generating cholesterol oxidation products, *i.e.*, oxysterols. The most common/abundant unsaturated or polyunsaturated CEs, such as cholesteryl linoleate [CE (18:2)], arachidonate [CE (20:4)], and docosahexaenoate [CE (22:6)], are most susceptible to oxidation because of the weak C−H double bond and readily form lipid peroxidation.[54] The OxCEs can also produce highly reactive end products, like malondialdehyde (MDA) or 4-hydroxy-2-nominal (4-HNE), which covalently modify proteins phosphatidylethanolamines (Figure 7). As CE (18:1), CE (18:2), and CE (22:6) have been significantly reduced in our study (Figure S4, Supporting Information), we suspect increased oxidation of CEs overall contributing to a decreased CE pool. It has been previously shown that EHDPP inhibits the mRNA of CYP7B1,[32] indicating more oxysterol conversion of cholesterol. Cholesterol is an essential lipid and an important component of the cell membrane. It is the precursor for the synthesis of steroids such as sex hormones (estrogen, testosterone, and progesterone) and corticosteroids (corticosterone, cortisol, cortisone, and aldosterone), bile acids, and vitamin D.[55] Therefore,

https://doi.org/10.1021/acs.est.2c03998
Environ. Sci. Technol. 2023, 57, 2006−2018

EHDPP may have additional adverse effects on the organisms, which require further research. In the present study, EHDPP treatment did not affect the cholesterol biosynthesis pathway but rather increased the cholesterol catabolism and oxysterol or bile acid metabolism pathway, as revealed by transcriptional analysis.

Interestingly, the expression of ACAT2, which is the hepatocyte-localized cholesterol-esterifying enzyme, was significantly increased. ACAT2 has been predominantly shown to form saturated and monounsaturated CEs, which may imply other mechanisms responsible for a decrease in unsaturated CE in our study. A similar alteration in cholesterol biosynthesis-related genes was noted earlier in other species, such as fish (Atlantic Cod liver)[56] and *in vitro* in chicken embryonic hepatocytes.[32] Our transcriptional assay indicated an increase in CYP27A1-mediated pathways, which suggests that EHDPP might have facilitated cholesterol efflux to oxysterols or bile acid, which needs further investigation. Moreover, we measured the ACAT1 mRNA and noted a decrease in its expression. The two isoform of ACAT, ACAT1 produces sterol esters, which are incorporated into cellular lipid droplets, while ACAT2 is involved in oxysterol synthesis.[57,58]

Moreover, the enhanced H_2O_2 production observed in the present study after EHDPP exposure indicates possible oxidative damage, namely, to the mitochondria, which is recognized as the primary cellular source of H_2O_2.[59] The increase in H_2O_2 emphasizes that EHDPP might be a potential mitochondrial toxicant and could induce detrimental effects on the mitochondria. Previous studies also report EHDPP-mediated attenuation of antioxidant enzymes such as superoxide dismutase and catalase in HepG2 cells, indicating potential effects on oxidative homeostasis.[60] Apparently, increased oxidative stress was supported by the upregulation of Nrf2 expression in the present study. Nrf2 is a transcriptional factor master regulator of antioxidant enzymes, which is activated upon redox imbalance.[61] It plays an essential role in the defense mechanism against oxidative stress and regulates metabolic pathways, including lipid metabolism.[62] Moreover, oxidative stress is one of the pathological mechanisms for the initiation and progression of various liver diseases, and it triggers hepatic damage by inducing the alteration of lipids and modulating pathways that control normal biological functions.[63] EHDPP exposure leads to an increase in the expression of PGC1α, which is activated in response to several environmental stresses and regulates energy metabolism, mitochondrial function, and biogenesis.[64] ROS production also triggers PGC1α expression, which, in turn, causes changes to mitochondrial biogenesis. It is also involved in the activation of hepatic gluconeogenesis and is a key regulator of bile acid biosynthesis.[65,66] An increase in PGC1α expression again indicates the disruption of mitochondrial function, ROS production, and impairment of energy homeostasis in HepG2 hepatospheroids after exposure to EHDPP.

In summary, the current study shows the effects of EHDPP exposure on hepatic lipid profiles using 3D hepatospheroid cell culture. We have noted a change in several major lipid classes, indicating possible hepatotoxic effects of EHDPP. Most phospholipids and TG species were upregulated, whereas CAR, sphingolipids, and CEs were downregulated along with transcriptional changes of key lipid metabolism-related genes. Our experimental observations suggest that EHDPP might have facilitated cholesterol efflux to oxysterols or bile acid through the PPAR-γ signaling pathway, which needs further investigations to delineate the possible causes, molecular mechanisms, and consequences on human health. This hepatotoxic potential of EHDPP raises serious concerns, considering that EHDPP is often detected at relatively high levels in environmental and human matrices.

Future studies should focus on the in-depth analysis of EHDPP-mediated adverse metabolic and reproductive pathologies in other human-relevant models to delineate the possible health hazards. The exposure concentrations in the present study might be directly relevant, for example, for the occupational/industrial or accidental exposure scenarios, and the relevance of the long-life environmental exposures should be further investigated. Environmental or occupational exposure to chemicals such as EHDPP might increase an individual's susceptibility to adverse metabolic phenotypes. Therefore, it is important to evaluate the EHDPP-associated risk of adverse metabolic effects such as lipid dysregulation, which eventually leads to the development and progression of NAFLD−NASH, insulin resistance, diabetes, *etc.*, especially in occupationally exposed populations and individuals with other risk factors.

■ ASSOCIATED CONTENT

Supporting Information

The Supporting Information is available free of charge at https://pubs.acs.org/doi/10.1021/acs.est.2c03998.

Additional information regarding lipid internal standards, chemical analysis, RT-qPCR primer sequence, and LC-MS/MS lipidomics analysis methods (PDF)

■ AUTHOR INFORMATION

Corresponding Author

Ludek Blaha − *RECETOX, Faculty of Science, Masaryk University, 61137 Brno, Czech Republic;* orcid.org/0000-0002-7314-7455; Email: ludek.blaha@recetox.muni.cz

Authors

Chander K. Negi − *RECETOX, Faculty of Science, Masaryk University, 61137 Brno, Czech Republic;* orcid.org/0000-0002-1568-3962

Darshak Gadara − *RECETOX, Faculty of Science, Masaryk University, 61137 Brno, Czech Republic;* orcid.org/0000-0002-3141-8990

Jiri Kohoutek − *RECETOX, Faculty of Science, Masaryk University, 61137 Brno, Czech Republic*

Lola Bajard − *RECETOX, Faculty of Science, Masaryk University, 61137 Brno, Czech Republic*

Zdeněk Spáčil − *RECETOX, Faculty of Science, Masaryk University, 61137 Brno, Czech Republic;* orcid.org/0000-0002-7505-4332

Complete contact information is available at: https://pubs.acs.org/10.1021/acs.est.2c03998

Funding

This project has received funding from the European Union's Horizon 2020 research and innovation programme under the Marie Sklodowska-Curie grant no. 859891. Authors also thank the RECETOX Research Infrastructure (no. LM2018121), financed by the Ministry of Education, Youth and Sports, and Operational Programme Research, Development, and Innovation- CETOCOEN Excellence (CZ.02.1.01/0.0/0.0/17_043/0009632) and CETOCOEN Plus (no. CZ.02.1.01/0.0/0.0/

15_003/0000469) for supportive background. This project was also supported from the European Union's Horizon 2020 research and innovation programme under grant agreements no. 857560. This publication reflects only the authors' view, and the European Commission is not responsible for any use that may be made of the information it contains.

Notes

The authors declare no competing financial interest.

■ ACKNOWLEDGMENTS

Figures were created using the paid version of Biorender.com.

■ REFERENCES

(1) Stapleton, H. M.; Klosterhaus, S.; Eagle, S.; Fuh, J.; Meeker, J. D.; Blum, A.; Webster, T. F. Detection of Organophosphate Flame Retardants in Furniture Foam and U.S. House Dust. *Environ. Sci. Technol.* **2009**, *43*, 7490−7495.

(2) Cristale, J.; Aragão Belé, T. G.; Lacorte, S.; Rodrigues de Marchi, M. R. Occurrence and Human Exposure to Brominated and Organophosphorus Flame Retardants via Indoor Dust in a Brazilian City. *Environ. Pollut.* **2018**, *237*, 695−703.

(3) Poma, G.; Glynn, A.; Malarvannan, G.; Covaci, A.; Darnerud, P. O. Dietary Intake of Phosphorus Flame Retardants (PFRs) Using Swedish Food Market Basket Estimations. *Food Chem. Toxicol.* **2017**, *100*, 1−7.

(4) Xu, F.; Tay, J. H.; Covaci, A.; Padilla-Sánchez, J. A.; Papadopoulou, E.; Haug, L. S.; Neels, H.; Sellström, U.; de Wit, C. A. Assessment of Dietary Exposure to Organohalogen Contaminants, Legacy and Emerging Flame Retardants in a Norwegian Cohort. *Environ. Int.* **2017**, *102*, 236−243.

(5) Zhao, L.; Jian, K.; Su, H.; Zhang, Y.; Li, J.; Letcher, R. J.; Su, G. Organophosphate Esters (OPEs)in Chinese Foodstuffs: Dietary Intake Estimation via a Market Basket Method, and Suspect Screening Using High-Resolution Mass Spectrometry. *Environ. Int.* **2019**, *128*, 343−352.

(6) Poma, G.; Sales, C.; Bruyland, B.; Christia, C.; Goscinny, S.; Van Loco, J.; Covaci, A. Occurrence of Organophosphorus Flame Retardants and Plasticizers (PFRs) in Belgian Foodstuffs and Estimation of the Dietary Exposure of the Adult Population. *Environ. Sci. Technol.* **2018**, *52*, 2331−2338.

(7) Hou, M.; Shi, Y.; Jin, Q.; Cai, Y. Organophosphate Esters and Their Metabolites in Paired Human Whole Blood, Serum, and Urine as Biomarkers of Exposure. *Environ. Int.* **2020**, *139*, No. 105698.

(8) Zhao, F.; Kang, Q.; Zhang, X.; Liu, J.; Hu, J. Urinary Biomarkers for Assessment of Human Exposure to Monomeric Aryl Phosphate Flame Retardants. *Environ. Int.* **2019**, *124*, 259−264.

(9) Zhao, F.; Wan, Y.; Zhao, H.; Hu, W.; Mu, D.; Webster, T. F.; Hu, J. Levels of Blood Organophosphorus Flame Retardants and Association with Changes in Human Sphingolipid Homeostasis. *Environ. Sci. Technol.* **2016**, *50*, 8896−8903.

(10) Zhao, F.; Chen, M.; Gao, F.; Shen, H.; Hu, J. Organophosphorus Flame Retardants in Pregnant Women and Their Transfer to Chorionic Villi. *Environ. Sci. Technol.* **2017**, *51*, 6489−6497.

(11) Noyes, P. D.; Haggard, D. E.; Gonnerman, G. D.; Tanguay, R. L. Advanced Morphological - Behavioral Test Platform Reveals Neurodevelopmental Defects in Embryonic Zebrafish Exposed to Comprehensive Suite of Halogenated and Organophosphate Flame Retardants. *Toxicol. Sci.* **2015**, *145*, 177−195.

(12) Jarema, K. A.; Hunter, D. L.; Shaffer, R. M.; Behl, M.; Padilla, S. Acute and Developmental Behavioral Effects of Flame Retardants and Related Chemicals in Zebrafish. *Neurotoxicol. Teratol.* **2015**, *52*, 194−209.

(13) Glazer, L.; Hawkey, A. B.; Wells, C. N.; Drastal, M.; Odamah, K. A.; Behl, M.; Levin, E. D. Developmental Exposure to Low Concentrations of Organophosphate Flame Retardants Causes Life-Long Behavioral Alterations in Zebrafish. *Toxicol. Sci.* **2018**, *165*, 487−498.

(14) Bajard, L.; Negi, C. K.; Mustieles, V.; Melymuk, L.; Jomini, S.; Barthelemy-Berneron, J.; Fernandez, M. F.; Blaha, L. Endocrine Disrupting Potential of Replacement Flame Retardants − Review of Current Knowledge for Nuclear Receptors Associated with Reproductive Outcomes. *Environ. Int.* **2021**, *153*, No. 106550.

(15) Klose, J.; Pahl, M.; Bartmann, K.; Bendt, F.; Blum, J.; Dolde, X.; Förster, N.; Holzer, A. K.; Hübenthal, U.; Keßel, H. E.; Koch, K.; Masjosthusmann, S.; Schneider, S.; Stürzl, L. C.; Woeste, S.; Rossi, A.; Covaci, A.; Behl, M.; Leist, M.; Tigges, J.; Fritsche, E. Neurodevelopmental Toxicity Assessment of Flame Retardants Using a Human DNT in Vitro Testing Battery. *Cell Biol. Toxicol.* **2021**, 781−807.

(16) Yan, S.; Wang, D.; Teng, M.; Meng, Z.; Yan, J.; Li, R.; Jia, M.; Tian, S.; Zhou, Z.; Zhu, W. Perinatal Exposure to 2-Ethylhexyl Diphenyl Phosphate (EHDPHP) Affected the Metabolic Homeostasis of Male Mouse Offspring: Unexpected Findings Help to Explain Dose- and Diet- Specific Phenomena. *J. Hazard. Mater.* **2020**, *388*, No. 122034.

(17) Sun, W.; Duan, X.; Chen, H.; Zhang, L.; Sun, H. Adipogenic Activity of 2-Ethylhexyl Diphenyl Phosphate via Peroxisome Proliferator-Activated Receptor γ Pathway. *Sci. Total Environ.* **2020**, *711*, No. 134810.

(18) Zhu, L.; Huang, X.; Li, Z.; Cao, G.; Zhu, X.; She, S.; Huang, T.; Lu, G. Evaluation of Hepatotoxicity Induced by 2-Ethylhexyldiphenyl Phosphate Based on Transcriptomics and Its Potential Metabolism Pathway in Human Hepatocytes. *J. Hazard. Mater.* **2021**, *413*, No. 125281.

(19) Zhao, F.; Li, Y.; Zhang, S.; Ding, M.; Hu, J. Association of Aryl Organophosphate Flame Retardants Triphenyl Phosphate and 2-Ethylhexyl Diphenyl Phosphate with Human Blood Triglyceride and Total Cholesterol Levels. *Environ. Sci. Technol. Lett.* **2019**, *6*, 532.

(20) Sen, P.; Qadri, S.; Luukkonen, P. K.; Ragnarsdottir, O.; McGlinchey, A.; Jäntti, S.; Juuti, A.; Arola, J.; Schlezinger, J. J.; Webster, T. F.; Orešič, M.; Yki-Järvinen, H.; Hyötyläinen, T. Exposure to Environmental Contaminants Is Associated with Altered Hepatic Lipid Metabolism in Non-Alcoholic Fatty Liver Disease. *J. Hepatol.* **2021**, 283.

(21) Negi, C. K.; Bajard, L.; Kohoutek, J.; Blaha, L. An Adverse Outcome Pathway Based in Vitro Characterization of Novel Flame Retardants-Induced Hepatic Steatosis. *Environ. Pollut.* **2021**, *289*, No. 117855.

(22) Bell, C. C.; Hendriks, D. F. G.; Moro, S. M. L.; Ellis, E.; Walsh, J.; Renblom, A.; Fredriksson Puigvert, L.; Dankers, A. C. A.; Jacobs, F.; Snoeys, J.; Sison-Young, R. L.; Jenkins, R. E.; Nordling, Å.; Mkrtchian, S.; Park, B. K.; Kitteringham, N. R.; Goldring, C. E. P.; Lauschke, V. M.; Ingelman-Sundberg, M. Characterization of Primary Human Hepatocyte Spheroids as a Model System for Drug-Induced Liver Injury, Liver Function and Disease. *Sci. Rep.* **2016**, *6*, No. 25187.

(23) Ramaiahgari, S. C.; Den Braver, M. W.; Herpers, B.; Terpstra, V.; Commandeur, J. N. M.; Van De Water, B.; Price, L. S. A 3D in Vitro Model of Differentiated HepG2 Cell Spheroids with Improved Liver-like Properties for Repeated Dose High-Throughput Toxicity Studies. *Arch. Toxicol.* **2014**, *88*, 1083−1095.

(24) Gong, X.; Lin, C.; Cheng, J.; Su, J.; Zhao, H.; Liu, T.; Wen, X.; Zhao, P. Generation of Multicellular Tumor Spheroids with Microwell-Based Agarose Scaffolds for Drug Testing. *PLoS One* **2015**, *10*, No. e0130348.

(25) Livak, K. J.; Schmittgen, T. D. Analysis of Relative Gene Expression Data Using Real-Time Quantitative PCR and the 2 C T Method. *Methods* **2001**, *25*, 402−408.

(26) Fahy, E.; Subramaniam, S.; Murphy, R. C.; Nishijima, M.; Raetz, C. R. H.; Shimizu, T.; Spener, F.; Van Meer, G.; Wakelam, M. J. O.; Dennis, E. A. Update of the LIPID MAPS Comprehensive Classification System for Lipids. *J. Lipid Res.* **2009**, S9−S14.

(27) Foulds, C. E.; Treviño, L. S.; York, B.; Walker, C. L. Endocrine-Disrupting Chemicals and Fatty Liver Disease. *Nat. Rev. Endocrinol.* **2017**, 445−457.

https://doi.org/10.1021/acs.est.2c03998
Environ. Sci. Technol. 2023, 57, 2006−2018

(28) Vinken, M. Adverse Outcome Pathways and Drug-Induced Liver Injury Testing. *Chem. Res. Toxicol.* **2015**, 1391−1397.
(29) Hu, W.; Gao, F.; Zhang, H.; Hiromori, Y.; Arakawa, S.; Nagase, H.; Nakanishi, T.; Hu, J. Activation of Peroxisome Proliferator-Activated Receptor Gamma and Disruption of Progesterone Synthesis of 2-Ethylhexyl Diphenyl Phosphate in Human Placental Choriocarcinoma Cells: Comparison with Triphenyl Phosphate. *Environ. Sci. Technol.* **2017**, *51*, 4061−4068.
(30) Fey, S. J.; Wrzesinski, K. Determination of Drug Toxicity Using 3D Spheroids Constructed From an Immortal Human Hepatocyte Cell Line. *Toxicol. Sci.* **2012**, *127*, 403.
(31) Bell, C. C.; Dankers, A. C. A.; Lauschke, V. M.; Sison-Young, R.; Jenkins, R.; Rowe, C.; Goldring, C. E.; Park, K.; Regan, S. L.; Walker, T.; Schofield, C.; Baze, A.; Foster, A. J.; Williams, D. P.; van de Ven, A. W. M.; Jacobs, F.; van Houdt, J.; Lähteenmäki, T.; Snoeys, J.; Juhila, S.; Richert, L.; Ingelman-Sundberg, M. Comparison of Hepatic 2D Sandwich Cultures and 3d Spheroids for Long-Term Toxicity Applications: A Multicenter Study. *Toxicol. Sci.* **2018**, *162*, 655−666.
(32) Shen, J.; Zhang, Y.; Yu, N.; Crump, D.; Li, J.; Su, H.; Letcher, R. J.; Su, G. Organophosphate Ester, 2-Ethylhexyl Diphenyl Phosphate (EHDPP), Elicits Cytotoxic and Transcriptomic Effects in Chicken Embryonic Hepatocytes and Its Biotransformation Profile Compared to Humans. *Environ. Sci. Technol.* **2019**, *53*, 2151−2160.
(33) Ballesteros-Gómez, A.; Erratico, C. A.; Van den Eede, N.; Ionas, A. C.; Leonards, P. E. G.; Covaci, A. In Vitro Metabolism of 2-Ethylhexyldiphenyl Phosphate (EHDPHP) by Human Liver Microsomes. *Toxicol. Lett.* **2015**, *232*, 203−212.
(34) Murosaki, S.; Lee, T. R.; Muroyama, K.; Shin, E. S.; Cho, S. Y.; Yamamoto, Y.; Lee, S. J. A Combination of Caffeine, Arginine, Soy Isoflavones, and l-Carnitine Enhances Both Lipolysis and Fatty Acid Oxidation in 3T3-L1 and HepG2 Cells in Vitro and in KK Mice in Vivo. *J. Nutr.* **2007**, *137*, 2252−2257.
(35) Noland, R. C.; Koves, T. R.; Seiler, S. E.; Lum, H.; Lust, R. M.; Ilkayeva, O.; Stevens, R. D.; Hegardt, F. G.; Muoio, D. M. Carnitine Insufficiency Caused by Aging and Overnutrition Compromises Mitochondrial Performance and Metabolic Control. *J. Biol. Chem.* **2009**, *284*, 22840−22852.
(36) Jun, D. W.; Cho, W. K.; Jun, J. H.; Kwon, H. J.; Jang, K. S.; Kim, H. J.; Jeon, H. J.; Lee, K. N.; Lee, H. L.; Lee, O. Y.; Yoon, B. C.; Choi, H. S.; Hahm, J. S.; Lee, M. H. Prevention of Free Fatty Acid-Induced Hepatic Lipotoxicity by Carnitine via Reversal of Mitochondrial Dysfunction. *Liver Int.* **2011**, *31*, 1315−1324.
(37) Li, J. L.; Wang, Q. Y.; Luan, H. Y.; Kang, Z. C.; Wang, C. B. Effects of L-Carnitine against Oxidative Stress in Human Hepatocytes: Involvement of Peroxisome Proliferator-Activated Receptor Alpha. *J. Biomed. Sci.* **2012**, *19*, No. 32.
(38) Puri, P.; Baillie, R. A.; Wiest, M. M.; Mirshahi, F.; Choudhury, J.; Cheung, O.; Sargeant, C.; Contos, M. J.; Sanyal, A. J. A Lipidomic Analysis of Nonalcoholic Fatty Liver Disease. *Hepatology* **2007**, *46*, 1081−1090.
(39) Rein-Fischboeck, L.; Haberl, E. M.; Pohl, R.; Feder, S.; Liebisch, G.; Krautbauer, S.; Buechler, C. Variations in Hepatic Lipid Species of Age-Matched Male Mice Fed a Methionine-Choline-Deficient Diet and Housed in Different Animal Facilities. *Lipids Health Dis.* **2019**, *18*, No. 172.
(40) Devaux, P. F. Static and Dynamic Lipid Asymmetry in Cell Membranes. *Biochemistry* **1991**, *30*, 1163−1173.
(41) van der Veen, J. N.; Kennelly, J. P.; Wan, S.; Vance, J. E.; Vance, D. E.; Jacobs, R. L. The Critical Role of Phosphatidylcholine and Phosphatidylethanolamine Metabolism in Health and Disease. *Biochim. Biophys. Acta, Biomembr.* **2017**, 1558−1572.
(42) Li, Z.; Agellon, L. B.; Allen, T. M.; Umeda, M.; Jewell, L.; Mason, A.; Vance, D. E. The Ratio of Phosphatidylcholine to Phosphatidylethanolamine Influences Membrane Integrity and Steatohepatitis. *Cell Metab.* **2006**, *3*, 321−331.
(43) Sekas, G.; Patton, G. M.; Lincoln, E. C.; Robins, S. J. Origin of Plasma Lysophosphatidylcholine: Evidence for Direct Hepatic Secretion in the Rat. *J. Lab. Clin. Med.* **1985**, *105*, 185−189.
(44) Kakisaka, K.; Cazanave, S. C.; Fingas, C. D.; Guicciardi, M. E.; Bronk, S. F.; Werneburg, N. W.; Mott, J. L.; Gores, G. J. Mechanisms of Lysophosphatidylcholine-Induced Hepatocyte Lipoapoptosis. *Am. J. Physiol.: Gastrointest. Liver Physiol.* **2012**, *302*, 77−84.
(45) Hollie, N. I.; Cash, J. G.; Matlib, M. A.; Wortman, M.; Basford, J. E.; Abplanalp, W.; Hui, D. Y. Micromolar Changes in Lysophosphatidylcholine Concentration Cause Minor Effects on Mitochondrial Permeability but Major Alterations in Function. *Biochim. Biophys. Acta, Mol. Cell Biol. Lipids* **2014**, *1841*, 888−895.
(46) Yamamoto, Y.; Sakurai, T.; Chen, Z.; Inoue, N.; Chiba, H.; Hui, S.-P. Lysophosphatidylethanolamine Affects Lipid Accumulation and Metabolism in a Human Liver-Derived Cell Line. *Nutrients* **2022**, *14*, No. 579.
(47) Epand, R. M. Features of the Phosphatidylinositol Cycle and Its Role in Signal Transduction. *J. Membr. Biol.* **2017**, *250*, 353−366.
(48) Burgess, J. W.; Boucher, J.; Neville, T. A. M.; Rouillard, P.; Stamler, C.; Zachariah, S.; Sparks, D. L. Phosphatidylinositol Promotes Cholesterol Transport and Excretion. *J. Lipid Res.* **2003**, *44*, 1355−1363.
(49) Merrill, A. H. Sphingolipid and Glycosphingolipid Metabolic Pathways in the Era of Sphingolipidomics. *Chem. Rev.* **2011**, 6387−6422.
(50) Lachkar, F.; Ferre, P.; Foufelle, F.; Papaioannou, A. Dihydroceramides: Their Emerging Physiological Roles and Functions in Cancer and Metabolic Diseases. *Am. J. Physiol.: Endocrinol. Metab.* **2021**, E122−E130.
(51) Krautbauer, S.; Meier, E. M.; Rein-Fischboeck, L.; Pohl, R.; Weiss, T. S.; Sigruener, A.; Aslanidis, C.; Liebisch, G.; Buechler, C. Ceramide and Polyunsaturated Phospholipids Are Strongly Reduced in Human Hepatocellular Carcinoma. *Biochim. Biophys. Acta, Mol. Cell Biol. Lipids* **2016**, *1861*, 1767−1774.
(52) Son, S. M.; Park, S. J.; Stamatakou, E.; Vicinanza, M.; Menzies, F. M.; Rubinsztein, D. C. Leucine Regulates Autophagy via Acetylation of the MTORC1 Component Raptor. *Nat. Commun.* **2020**, *11*, No. 3148.
(53) Khan, S. R.; Manialawy, Y.; Obersterescu, A.; Cox, B. J.; Gunderson, E. P.; Wheeler, M. B. Diminished Sphingolipid Metabolism, a Hallmark of Future Type 2 Diabetes Pathogenesis, Is Linked to Pancreatic β Cell Dysfunction. *iScience* **2020**, *23*, No. 101566.
(54) Hutchins, P. M.; Murphy, R. C. Cholesteryl Ester Acyl Oxidation and Remodeling in Murine Macrophages: Formation of Oxidized Phosphatidylcholine. *J. Lipid Res.* **2012**, *53*, 1588−1597.
(55) Wang, H. H.; Garruti, G.; Liu, M.; Portincasa, P.; Wang, D. Q. H. Cholesterol and Lipoprotein Metabolism and Atherosclerosis: Recent Advances in Reverse Cholesterol Transport. *Ann. Hepatol.* **2017**, *16*, s27−s42.
(56) Aluru, N.; G Hallanger, I.; McMonagle, H.; Harju, M. Hepatic Gene Expression Profiling of Atlantic Cod (*Gadus morhua*) Liver after Exposure to Organophosphate Flame Retardants Revealed Altered Cholesterol Biosynthesis and Lipid Metabolism. *Environ. Toxicol. Chem.* **2021**, *40*, 1639−1648.
(57) Liu, J.; Chang, C. C. Y.; Westover, E. J.; Covey, D. F.; Chang, T. Y. Investigating the Allosterism of Acyl-CoA:Cholesterol Acyltransferase (ACAT) by Using Various Sterols: In Vitro and Intact Cell Studies. *Biochem. J.* **2005**, *391*, 389−397.
(58) Cases, S.; Novak, S.; Zheng, Y.-W.; Myers, H. M.; Lear, S. R.; Sande, E.; Welch, C. B.; Lusis, A. J.; Spencer, T. A.; Krause, B. R.; Erickson, S. K.; Farese, R. V. ACAT-2, A Second Mammalian Acyl-CoA:Cholesterol Acyltransferase. *J. Biol. Chem.* **1998**, *273*, 26755−26764.
(59) Boveris, A.; Cadenas, E. Mitochondrial Production of Hydrogen Peroxide Regulation by Nitric Oxide and the Role of Ubisemiquinone. *IUBMB Life* **2001**, *50*, 245−250.
(60) Zhou, Y.; Liao, H.; Yin, S.; Wang, P.; Ye, X.; Zhang, J. Aryl-, Halogenated- and Alkyl- Organophosphate Esters Induced Oxidative Stress, Endoplasmic Reticulum Stress and NLRP3 Inflammasome Activation in HepG2 Cells. *Environ. Pollut.* **2022**, No. 120559.

https://doi.org/10.1021/acs.est.2c03998
Environ. Sci. Technol. 2023, 57, 2006−2018

(61) Negi, C. K.; Jena, G. Nrf2, a Novel Molecular Target to Reduce Type 1 Diabetes Associated Secondary Complications: The Basic Considerations. *Eur. J. Pharmacol.* **2019**, *843*, 12−26.
(62) Huang, J.; Tabbi-Anneni, I.; Gunda, V.; Wang, L. Transcription Factor Nrf2 Regulates SHP and Lipogenic Gene Expression in Hepatic Lipid Metabolism. *Am. J. Physiol.: Gastrointest. Liver Physiol.* **2010**, *299*, G1211.
(63) Li, S.; Tan, H. Y.; Wang, N.; Zhang, Z. J.; Lao, L.; Wong, C. W.; Feng, Y. The Role of Oxidative Stress and Antioxidants in Liver Diseases. *Int. J. Mol. Sci.* **2015**, *16*, 26087.
(64) Lin, J.; Handschin, C.; Spiegelman, B. M. Metabolic Control through the PGC-1 Family of Transcription Coactivators. *Cell Metab.* **2005**, 361−370.
(65) Puigserver, P.; Spiegelman, B. M. Peroxisome Proliferator-Activated Receptor-γ Coactivator 1α (PGC-1α): Transcriptional Coactivator and Metabolic Regulator. *Endocr. Rev.* **2003**, 78−90.
(66) Shin, D. J.; Campos, J. A.; Gil, G.; Osborne, T. F. PGC-1α Activates CYP7A1 and Bile Acid Biosynthesis. *J. Biol. Chem.* **2003**, *278*, 50047−50052.

https://doi.org/10.1021/acs.est.2c03998
Environ. Sci. Technol. 2023, 57, 2006−2018